Anthrax Vaccine Powder Formulations for Nasal Mucosal Delivery

GE JIANG,[1] SANGEETA B. JOSHI,[2] LAURA J. PEEK,[2] DUANE T. BRANDAU,[2] JUAN HUANG,[1] MATTHEW S. FERRITER,[1] WENDY D. WOODLEY,[1] BRANDI M. FORD,[1] KEVIN D. MAR,[1] JOHN A. MIKSZTA,[1] C. ROBIN HWANG,[1] ROBERT ULRICH,[3] NOEL G. HARVEY,[1] C. RUSSELL MIDDAUGH,[2] VINCENT J. SULLIVAN[1]

[1]BD Technologies, 21 Davis Dr., RTP, North Carolina 27709

[2]Department of Pharmaceutical Chemistry, University of Kansas, 2095 Constant Ave., Lawrence, Kansas 66047

[3]US Army Medical Research Institute of Infectious Diseases, 1425 Porter St., Fort Detrick, Maryland 21702

Received 4 March 2005; revised 23 June 2005; accepted 4 August 2005

Published online in Wiley InterScience (www.interscience.wiley.com). DOI 10.1002/jps.20484

ABSTRACT: Anthrax remains a serious threat worldwide as a bioterror agent. A second-generation anthrax vaccine currently under clinical evaluation consists of a recombinant Protective Antigen (rPA) of *Bacillus anthracis*. We have previously demonstrated that complete protection against inhalational anthrax can be achieved in a rabbit model, by intranasal delivery of a powder rPA formulation. Here we describe the preformulation and formulation development of such powder formulations. The physical stability of rPA was studied in solution as a function of pH and temperature using circular dichroism (CD), and UV-visible absorption and fluorescence spectroscopies. Extensive aggregation of rPA was observed at physiological temperatures. An empirical phase diagram, constructed using a combination of CD and fluorescence data, suggests that rPA is most thermally stable within the pH range of 6–8. To identify potential stabilizers, a library of GRAS excipients was screened using an aggregation sensitive turbidity assay, CD, and fluorescence. Based on these stability profiles, spray freeze-dried (SFD) formulations were prepared at pH 7–8 using trehalose as stabilizer and a CpG-containing oligonucleotide adjuvant. SFD formulations displayed substantial improvement in storage stability over liquid formulations. In combination with noninvasive intranasal delivery, such powder formulations may offer an attractive approach for mass biodefense immunization. J Pharm Sci 95:80–96, 2006

Keywords: anthrax; recombinant protective antigen; nasal; powder formulation; stability

INTRODUCTION

Anthrax, the zoonotic disease caused by the Gram-positive spore-forming bacterium, *Bacillus anthracis*, can infect humans via cutaneous, gastrointestinal, and pulmonary routes. The inhaled form is of particular concern considering its demonstrated use as a bioweapon.[1–4] Inhalational anthrax is difficult to diagnose and effectively treat with antibiotics; therefore, prophylactic vaccination is critical to elicit protection for individuals at risk of exposure.[5,6]

B. anthracis produces a three component exotoxin (anthrax toxin complex), which consists of protective antigen (PA, 83 kDa), edema factor (EF, 89 kDa), and lethal factor (LF, 90 kDa).[7–9] While all three proteins are nontoxic individually, the combination of PA and LF (designated lethal toxin) causes systemic shock and death associated with hyperoxidative burst and cytokine release from macrophages.[10,11] A combination of PA and EF,

Correspondence to: Vincent J. Sullivan (Telephone: 919-597-6173; Fax: 919-597-6402; E-mail: vince_Sullivan@bd.com)

Journal of Pharmaceutical Sciences, Vol. 95, 80–96 (2006)

Report Documentation Page

Form Approved
OMB No. 0704-0188

1. REPORT DATE	2. REPORT TYPE	3. DATES COVERED
1 JAN 06	**N/A**	

4. TITLE AND SUBTITLE	5a. CONTRACT NUMBER
Anthrax vaccine powder formulations for nasal mucosal delivery, Journal of Pharmaceutical Science 95:80 - 96	5b. GRANT NUMBER
	5c. PROGRAM ELEMENT NUMBER

6. AUTHOR(S)	5d. PROJECT NUMBER
Jiang /G Joshi, SB Peek, LJ Brandau, DT Huang, J Ferriter, M Woodley, WD Ford, BM Mar, KD Mikszta, JA Huang, CR Ulrich, R Harvey, NG Middaugh, CR Sullivan, VJ	5e. TASK NUMBER
	5f. WORK UNIT NUMBER

7. PERFORMING ORGANIZATION NAME(S) AND ADDRESS(ES)	8. PERFORMING ORGANIZATION REPORT NUMBER
United States Army Medical Research Institute of Infectious Diseases, Fort Detrick, MD	

9. SPONSORING/MONITORING AGENCY NAME(S) AND ADDRESS(ES)	10. SPONSOR/MONITOR'S ACRONYM(S)
	11. SPONSOR/MONITOR'S REPORT NUMBER(S)

12. DISTRIBUTION/AVAILABILITY STATEMENT

Approved for public release, distribution unlimited.

13. SUPPLEMENTARY NOTES

The original document contains color images.

14. ABSTRACT

Anthrax remains a serious threat worldwide as a bioterror agent. A second-generation anthrax vaccine currently under clinical evaluation consists of a recombinant Protective Antigen (rPA) of Bacillus anthracis. We have previously demonstrated that complete protection against inhalational anthrax can be achieved in a rabbit model, by intranasal delivery of a powder rPA formulation. Here we describe the preformulation and formulation development of such powder formulations. The physical stability of rPA was studied in solution as a function of pH and temperature using circular dichroism (CD), and UV-visible absorption and fluorescence spectroscopies. Extensive aggregation of rPA was observed at physiological temperatures. An empirical phase diagram, constructed using a combination of CD and fluorescence data, suggests that rPA is most thermally stable within the pH range of 6-8. To identify potential stabilizers, a library of GRAS excipients was screened using an aggregation sensitive turbidity assay, CD, and fluorescence. Based on these stability profiles, spray freeze-dried (SFD) formulations were prepared at pH 7-8 using trehalose as stabilizer and a CpG-containing oligonucleotide adjuvant. SFD formulations displayed substantial improvement in storage stability over liquid formulations. In combination with noninvasive intranasal delivery, such powder formulations may offer an attractive approach for mass biodefense immunization.

15. SUBJECT TERMS

16. SECURITY CLASSIFICATION OF:			17. LIMITATION OF ABSTRACT	18. NUMBER OF PAGES	19a. NAME OF RESPONSIBLE PERSON
a. REPORT	b. ABSTRACT	c. THIS PAGE			
unclassified	**unclassified**	**unclassified**	**SAR**	**17**	

known as edema toxin, induces an increase in intracellular cAMP and also elicits edema at the site of infection.[12,13] PA plays an essential role in anthrax pathogenesis, involving transport of LF and EF into the cytoplasm.[4,14,15] PA is also the primary immunogenic molecule that confers protection against anthrax.[16,17] The current licensed anthrax vaccines for human use are produced from the sterile culture supernatant fraction of *B. anthracis* and are adsorbed on aluminum hydroxide for intramuscular (IM) injection[18] in the United States and precipitated with aluminum phosphate for subcutaneous (SC) injection in the United Kingdom.[19] These vaccines contain varying amounts of natural PA and also small amounts of LF and EF.[20] A limited duration of protection and a consequent need for frequent boosts to maintain immunity have resulted in recent efforts to develop alternative vaccines such as those that employ recombinant PA (rPA) to improve the immunogenicity, safety, and pharmaceutical consistency.[2,21,22]

A second generation anthrax vaccine consisting of a recombinantly produced PA antigen is currently under clinical investigation where it is being administered by IM injection.[23] Alternative routes other than IM could also be effective. Delivery of vaccine to the respiratory mucosa may offer an attractive alternative to parenteral delivery for protection against pulmonary anthrax infection. Intranasal (IN) immunization is efficient at eliciting mucosal immunity in the lungs,[24–26] and has been shown in animals to be an effective means of immunizing against pulmonary anthrax infection.[2] IN vaccination offers advantages, as it is noninvasive route of delivery, with potential for self-administration. Nasal immunization with rPA could be further facilitated by the use of stable powder formulations delivered via a unit dose, disposable device. Nasal powder delivery may have several advantages over conventional liquid formulations for parenteral routes including protection from hydrolysis in bulk solution, potential elimination of the need for refrigeration, increased portability, and better suitability for mass immunization campaigns through an all-in-one prefilled device.

Previously, we reported that IN delivery of a powder formulation of rPA provides complete protection against inhalational anthrax in a rabbit model.[27] These results are summarized in Table 1. *In vivo* protective efficacy was reflected by animal survival after aerosol anthrax spore challenge. The IN powders elicited similar or slightly higher protection compared to liquid formulations administered IM or IN (Tab. 1). In the present study, we describe the preformulation work, including investigation of the biophysical stability of rPA and the subsequent formulation and characterization of such IN rPA vaccine powders. The stability of rPA in solution as a function of pH and temperature was assessed and interpreted by an empirical phase diagram approach.[28] In addition, stabilizers were examined in order to identify a range of optimal formulation conditions. Stabilizers and processing on the intrinsic stability of rPA as well as on its storage stability under accelerated conditions was also investigated.

Table 1. Protective Effect from Intranasal Dry Powder Formulations in Rabbits Receiving Anthrax Inhalational Challenge (Each Rabbit Received 50 μg of rPA, $n = 6$ for Each Group)[27]

Formulation and Administration Route	Animal Survival (%)
Positive control (rPA/CpG liquid, IM)	83
rPA/CpG liquid, IN	67
rPA/CpG/trehalose SFD powder, IN	83
rPA/CpG/trehalose SFD powder + chitosan, IN	100
rPA/CpG/trehalose FD powder, IN	100
rPA/CpG/trehalose FD powder + chitosan, IN	100
Negative control (CpG)	0

MATERIALS AND METHODS

Materials

rPA was obtained from two different sources, the US Army Medical Research Institute of Infectious Diseases (USAMRIID, Fredrick, MD) and List Biological Laboratories (Campbell, CA). rPA from both sources was expressed and purified from *Bacillus anthracis* and was equivalent based on the criteria of size exclusion chromatography (SEC) and SDS–PAGE analysis. The CpG-containing oligonucleotide (#1826, TCCATGACGTTCCTGACGTT) was purchased from Proligo, LLC (Boulder, CO). Chitosan (MW 50000–190000) was purchased from Sigma (St. Louis, MO). CpG was chosen because it has been shown to be an effective mucosal adjuvant in previous preclinical studies.[29] All other reagents including buffers and salts were purchased from Sigma (St. Louis, MO) and were of analytical grade.

Experimental Methods

Physical Characterization of rPA Stability

rPA Sample Preparation. rPA solution was prepared at a concentration of 2.4 μM for UV absorption and CD studies or 1.2 μM for fluorescence studies in 50 mM citrate phosphate buffer containing 0.1 M NaCl at six different pH values from 3 to 8 at one pH unit intervals.

UV Optical Density Measurements. The effect of temperature on rPA aggregation was determined by monitoring turbidity at 360 nm at each pH value using an Agilent 8453 UV-Visible spectrophotometer over a temperature range of 10–90°C at 2.5°C intervals as described previously.[28] A 5-min equilibration time was employed at each temperature interval to ensure equilibrium conditions.

Circular Dichroism (CD). CD studies were performed as described earlier[30] using a Jasco J-810 spectropolarimeter equipped with a 6-position Peltier temperature controller to measure changes in the secondary structure of rPA as a function of temperature. Each sample was examined in a 0.1 cm pathlength cuvette sealed with a Teflon stopper, and the CD signal of rPA at 222 nm was monitored as a function of temperature from 10°C to 90°C, collecting data every 0.5°C. The CD signal was converted to molar ellipticity using the Jasco Spectra Manager software.

Intrinsic Tryptophan (Trp) Fluorescence. Intrinsic fluorescence measurements were performed as described earlier[30] to assess perturbations in the tertiary structure of rPA as a function of temperature and pH. Fluorescence emission spectra of rPA (1.2 μM) were recorded from 10 to 85°C using a PTI Quanta Master Spectrofluorometer equipped with a turreted, four-cell thermostatically controlled holder. An excitation wavelength of 295 nm (>95% Trp Emission) was employed and emission spectra were collected from 305 to 440 nm. Excitation and emission slits were set at 4 nm and a 1 cm pathlength quartz cuvette was used in all experiments. Spectra were collected at 2.5°C intervals with a 5-min equilibration time at each temperature. Buffer baselines were subtracted from each spectrum prior to data analysis using Felix™ (PTI) software. Emission peak positions were obtained by a "center of spectral mass" method, which calculates the zero moment of the entire spectral curve from 305 to 440 nm. Typically, the "center of spectral mass" values do not correspond to observed peak maxima (λ_{max}), but do accurately reflect the trend in actual peak position changes.

ANS Dye Binding Studies. The apolar dye, 8-Anilino-1-naphthalene sulfonate (ANS), often binds to hydrophophic regions on proteins as their conformation is altered. This usually results in enhanced fluorescence as well as a blue shift in the emission peak position. Thus, the association of ANS with rPA (1.2 μM) was monitored as a function of temperature (10–85°C) and pH (3–8) using a PTI Quanta Master Spectrofluorometer. ANS was added in a 20-fold molar excess over rPA. An excitation wavelength of 375 nm was used, and spectra were collected from 400 to 600 nm. The temperature ramping profile and instrument settings were the same as those used for the intrinsic Trp fluorescence experiments. Blanks of buffer containing ANS were subtracted from each spectrum prior to data analysis.

Constructing Empirical Phase Diagram

An empirical phase diagram was constructed as described previously[28] but in this case using CD molar ellipticity, intrinsic Trp fluorescence emission peak center of mass, and ANS fluorescence intensity data sets. All calculations were performed using the software Mathematica (Wolfram Research, Champaign, IL). The theory and calculation process are described in more detail elsewhere.[28] Briefly, experimental data sets are represented as n-dimensional vectors in a temperature/pH phase space, where n refers to the number of variables (different types of data) included in the calculation. The data from each technique at individual values of pH and temperature serve as the bases for the individual vector's components. An $n \times n$ density matrix combining all of the individual vectors is then constructed and n sets of eigenvalues and eigenvectors of the density matrix are calculated. The complete data set is subsequently truncated and re-expanded into three dimensions consisting of eigenvectors corresponding to the three largest eigenvalues. The phase diagram is then generated using vectors reconstructed in these three dimensions employing an arbitrary red/green/blue color scheme.

Screening for Stabilizers

An initial high-throughput screen for stabilizers was performed utilizing the susceptibility of rPA to aggregation by monitoring the turbidity of the solution with an optical density measurement at 360 nm using a 96-well plate reader (BMG Labtechnologies, Offenburg, Germany). To identify potential stabilizers, more than 30 "Generally Regarded As Safe" (GRAS) excipients including buffers, sugars, amino acids, and surfactants were screened for their ability to inhibit the aggregation of rPA. In a 96-well plate, rPA (0.25 mg/mL) was added to wells containing each compound from the GRAS library at selected concentrations in citrate–phosphate buffer at pH 5. The samples were incubated at 37°C, and the optical density of the solutions in each well was monitored at 360 nm (OD_{360}) for 70 min with readings obtained at 5-min intervals. Controls of rPA solution without excipient were examined simultaneously. The final OD_{360} observed at 70 min was used to calculate the percent inhibition of rPA aggregation produced by each compound.

Several effective inhibitors of rPA aggregation were further studied to determine their effect on the conformational stability of rPA upon thermal denaturation, using the CD and intrinsic fluorescence methods described previously. Titration experiments were performed with the selected stabilizer by monitoring turbidity, as described above, to obtain the optimal concentration range of the stabilizer.

Formulation of Anthrax Dry Powder Vaccine

The anthrax dry powder was formulated by freeze drying (FD) or spray freeze drying (SFD) with rPA, trehalose, and an adjuvant comprising the CpG-containing oligonucleotide (#1826, TCCATGACGTTCCTGACGTT) (abbreviated herein as CpG). rPA was supplied at pH 8 in either ammonium acetate solution (USAMRIID material) or in a freeze dried form (List Lab material) containing HEPES buffer salts. The rPA solution was mixed with CpG and trehalose solutions to obtain the final concentrations of 0.5 mg/mL rPA, 0.5 mg/mL CpG, 99.0 mg/mL trehalose (with trace amount of salts from the rPA material). Part of this solution was stored at −70°C for stability testing and the remainder was aliquotted for FD and SFD. To produce SFD powder, the solution was first sprayed into liquid nitrogen using a BD Accuspray® nozzle. The frozen particles obtained were collected into lyophilization vials and then transferred to a freeze drier (Dura-Stop/Dura-Dry, FTS Systems, Stonebridge, NY) precooled to −40°C. Finally, both FD and SFD samples underwent a lyophilization cycle in which the primary drying was performed at −10°C (shelf temperature) for 16 h, followed by a gradual ramping of the shelf temperature to 20°C for secondary drying. The vials were stoppered under a nitrogen backfill. The FD cake was milled by ball milling (Wig-L-Bug Grinding Mill, Reflex Analytical Corp, Ridgewood, NJ) for 1 min at 3000 rpm to generate the final powder. These rPA/CpG/trehalose powders can be filled into the capsule of an IN delivery device previously described.[27,31] Additionally, to determine if a bioadhesive further enhances immunity, aliquots of the above powders were blended with a chitosan powder prior to device filling.

Determination of rPA Stability during the SFD Process

The integrity of rPA throughout the SFD process was determined by SDS–PAGE under both reducing and nonreducing conditions and by SEC-HPLC. Samples were collected at each step of the SFD process, that is, after mixing of rPA with CpG and trehalose, after the solution was sprayed from the nozzle, after the sprayed droplets were frozen in liquid nitrogen, and after the final lyophilization. The final dried powder was also reconstituted in water for SEC-HPLC analysis for comparison to freshly prepared rPA/CpG/trehalose solution.

Storage Stability Studies of Anthrax Vaccine Formulations under Accelerated Conditions

The SFD anthrax vaccine powder was aliquotted into 2 mL serum vials (Wheaton, Millville, NJ) in a dry box (Terra Universal, Anaheim, CA) under nitrogen purge. Prior to filling with powder samples, rubber stoppers and glass vials remained overnight under nitrogen purge in a dry box. Each vial contained ~25 mg of powder. The vials were sealed with rubber stoppers and aluminum crimp seals. The liquid formulation containing the same composition as the SFD powder was also included in the stability study. After storage at 25°C or 40°C, powder samples were reconstituted in ~0.25 mL water for analysis. Ten microliters of each sample were used for SDS–PAGE analysis and the remaining solution was filtered through a 0.22 μm centrifugal filter (Millipore, Bedford, MA) prior to SEC-HPLC.

Size Exclusion Chromatography (SEC)

SEC was performed using a Waters HPLC instrument equipped with a binary pump (Waters 1525, Milford, MA), an autosampler (Waters 717 plus), and UV spectrophotometric detector (Waters 2487) interfaced to a Waters Breeze software package. Two size exclusion columns were used (Shodex®, JM Science, Inc., Grand Island, NY), a KW-803 (cutoff 700000) column coupled to a KW-802.5 (cutoff 150000) column to enhance resolution. Samples (75 μL) were analyzed by UV detection ($\lambda = 220$ nm) employing a mobile phase consisting of 50 mM NaCl, 5 mM HEPES, 200 ppm sodium azide, and a flow rate of 0.5 mL/min. After passing through the UV detector, the samples were additionally analyzed using a multi-angle light scattering detector (Wyatt Technology Opitilab DSP, Santa Barbara, CA) for molecular weight measurement. The light scattering data were analyzed using Wyatt Astra software.

SDS–PAGE

SDS–PAGE was performed with a precast NuPAGE 4–20% TrisGly gel (Invitrogen, Carlsbad, CA). Protein samples and standards were mixed with 2× Tris-Glycine SDS sample buffer (Invitrogen) containing 2% SDS. For reducing conditions, dithiothreitol (1 M) and 2-Mercaptoethanol were added at 5% (v/v) each in the samples. Samples were incubated for 8 min at 95°C, and electrophoresis was performed at a constant voltage of 125 V and 8 mA. The gel was stained with Colloidal Blue (Invitrogen) and destained with distilled water.

RESULTS AND DISCUSSION

Physical Characterization of rPA Stability as a Function of pH and Temperature

The effect of pH and temperature on the physical stability of rPA was analyzed using a number of biophysical approaches. First, aggregation of rPA was both temperature- and pH-dependent as observed by monitoring the turbidity at 360 nm (Fig. 1A). Between pH 4 and 7, the temperature at which aggregation began increased with pH. At pH 8, aggregation of rPA began at slightly lower temperature than at pH 7 with more substantial reductions in aggregation onset temperature at lower pH. Additionally, the extent of temperature-induced aggregation as indicated by the maximum OD was lower for rPA at pH 7–8 than at pH 4–6. The subsequent decline of OD is indicative of extensive protein precipitation. At pH 7–8, turbidity onset occurred at higher temperatures suggesting that rPA is thermally more stable in this pH range. At pH 3, aggregation of rPA was only detected at temperatures above 80°C, indicating that the aggregation mechanism may differ from that at pH 4–8.

The CD spectra of rPA display minima at about 206–208 nm with a shoulder at 216–217 nm at all pH values (Fig. 1B). This suggests that rPA primarily consists of a mixture of secondary structure moieties (e.g., α-helix and β-sheet). The calculated secondary structure from the CD spectra is comparable to that of PA reported previously.[32] At 10°C, the CD spectrum of rPA at pH 3 remained distinct from that at other pH values with a significantly lower molar ellipticity, indicating that the secondary structure of rPA in solution is altered at very low pH. The secondary structure of rPA underwent significant pH and temperature-dependent transitions, suggesting a loss of secondary structure as evidenced by a decrease in the negative ellipticity (Fig. 1C). The opposite is seen, however, at pH 3. Thermally induced ellipticity changes occured at significantly lower temperatures at acidic pH values (e.g., pH 4) suggesting that rPA is structurally more labile in an acidic environment. The different behavior seen at pH 3 suggests that rPA undergoes a different type of structural alteration compared to that occurring at higher pH values (Fig. 1C). This is consistent with the altered CD spectrum seen even at low temperature at this pH (Fig. 1B). No major thermally induced changes were seen at pH 7–8, implying higher thermal stability under these conditions; this is also consistent with the temperature/turbidity studies (Fig. 1A).

Intrinsic (Trp) fluorescence studies were performed to detect changes in the tertiary structure of rPA. The shift in fluorescence emission peak position as a function of temperature at various pH values is shown in Figure 1D. At all pH values, the peak position displays a red shift at elevated temperatures. This corresponds to an increase in exposure of the Trp residues to a more polar environment implying protein unfolding. Again, the onset temperature for red shift increased with increasing pH. Thus, these experiments also suggest that the most stable environment for rPA is within the pH range of 7–8.

At pH 4 and 5, changes in the tertiary structure of rPA were detected in fluorescence spectra at

approximately 20–25°C. In contrast, CD thermal transitions began at higher temperatures, that is, 33°C and 37°C for pH 4 and 5, respectively (Tab. 2). This suggests that a range of temperatures exist in which rPA possesses a retention of pronounced secondary structure and compactness, but a partial loosening of the native, tightly packed tertiary structure. Similar characteristics are also observed for rPA at pH 6–8. This suggests the appearance of molten globule-like states[33,34] between these temperatures. Such states are often prone to protein aggregation.[35,36] The turbidity profiles for rPA (Fig. 1A) support this idea since the temperature at which aggregation begins for rPA at pH 4–8 falls within the temperature range of molten globule-like states as determined by intrinsic fluorescence and CD.

The hydrophobic dye, ANS, was utilized as an extrinsic fluorescent probe to further investigate alterations in rPA tertiary structure. As a protein begins to unfold, the increased accessibility of the dye to the protein's apolar interior often results in an enhanced fluorescence signal. In some cases, however, the negative charge on ANS is also thought to be involved in its interaction with proteins. ANS is also believed to have a much stronger affinity for protein "molten globule states" than for native and severely structurally disrupted conformational states.[37–39] The change in ANS fluorescence intensity as a function of

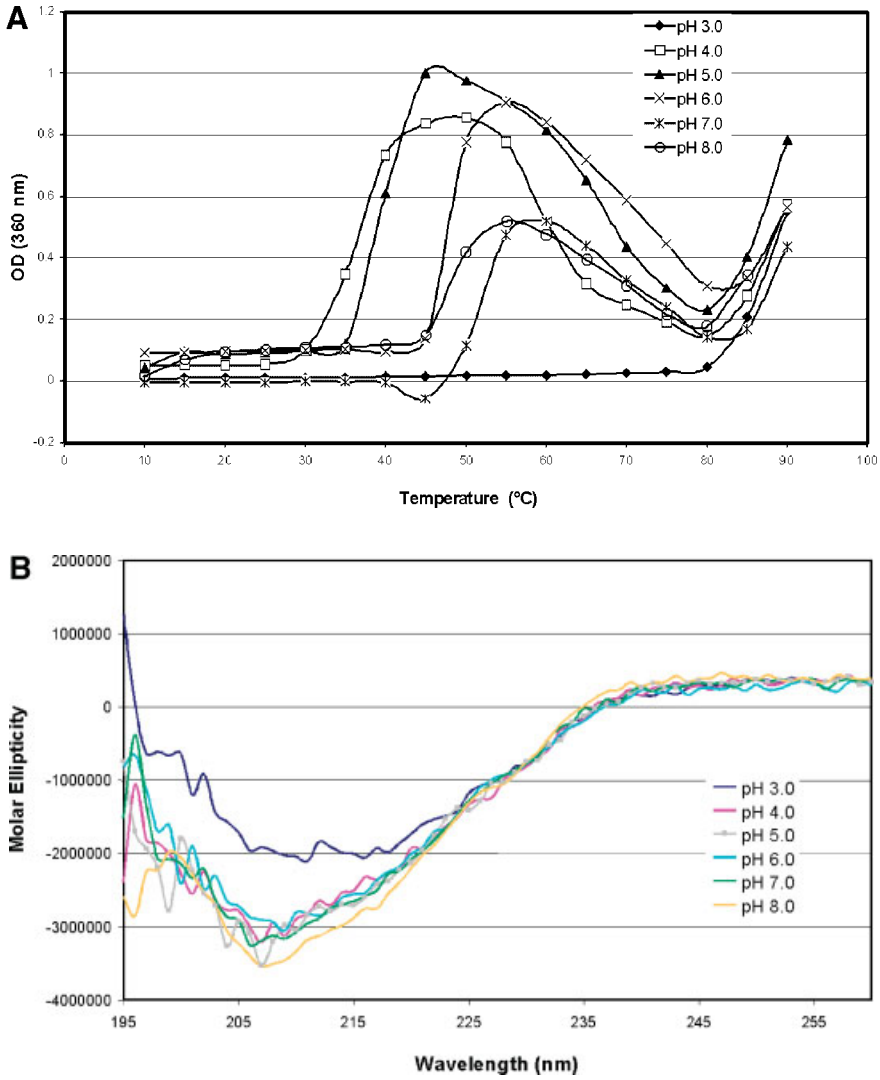

Figure 1. Physical stability of rPA as a function of pH and temperature in citrate–phosphate buffer as determined by using optical density to detect insoluble aggregates (A); CD spectra of rPA at 10°C (B); CD thermal melts monitored at 222 nm (C); intrinsic Trp fluorescence spectra center of mass (D); ANS dye binding fluorescence intensity (E).

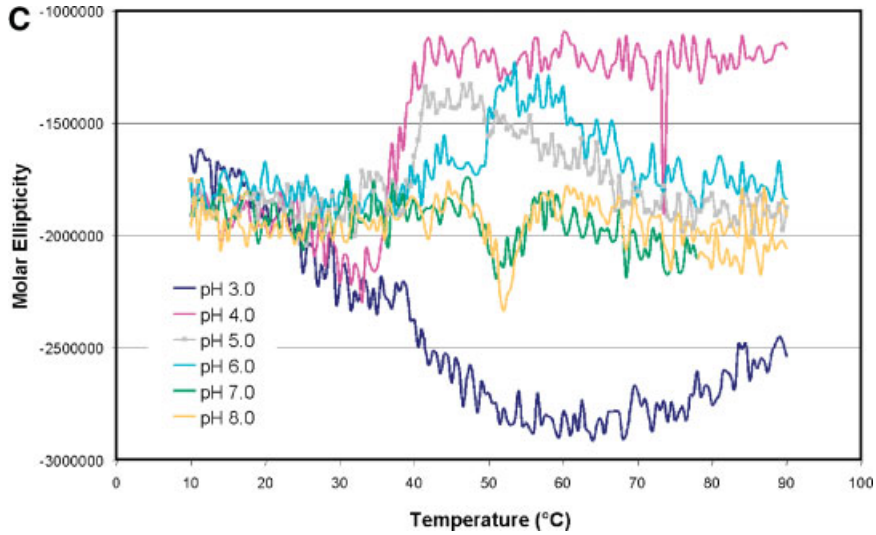

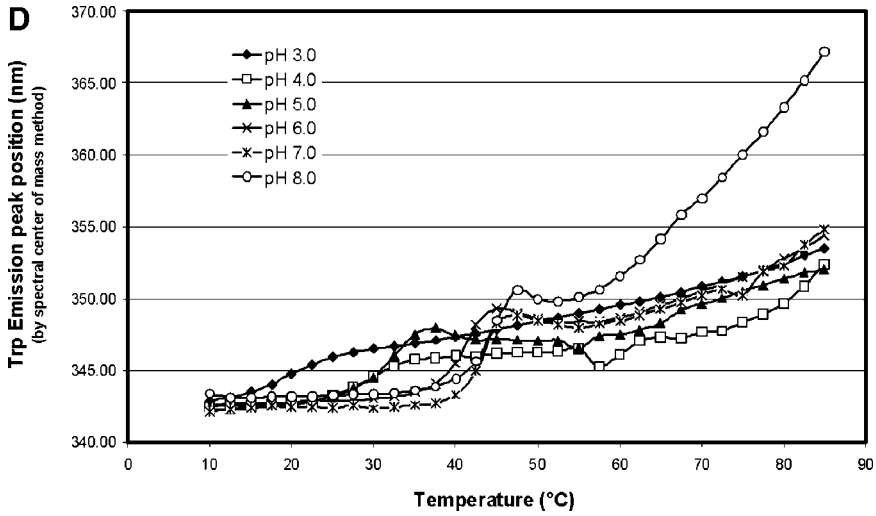

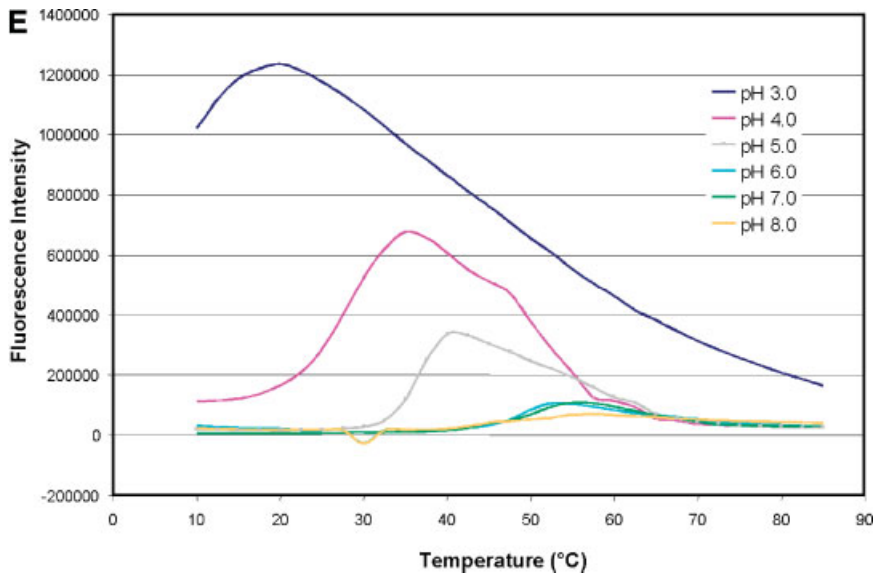

Figure 1. (*Continued*)

Table 2. Thermal Transition Onset Temperatures of rPA Characterized by Optical Density (OD_{360nm}), CD, Intrinsic Trp Fluorescence, and ANS Dye-Binding Fluorescence

	Biophysical Approaches			
PH	OD_{360}	CD	Trp Fluorescence	ANS Dye-Binding Fluorescence
3	81.7°C	16.4°C	16.5°C	10.0°C
4	30.4°C	32.8°C	22.5°C	21.5°C
5	36.4°C	36.5°C	25.2°C	30.1°C
6	43.7°C	43.0°C	37.5°C	42.3°C
7	46.8°C	48.0°C	42.1°C	45.0°C
8	47.9°C	46.3°C	40.0°C	40.8°C

Standard errors for all runs were 0 ± 0.5°C.

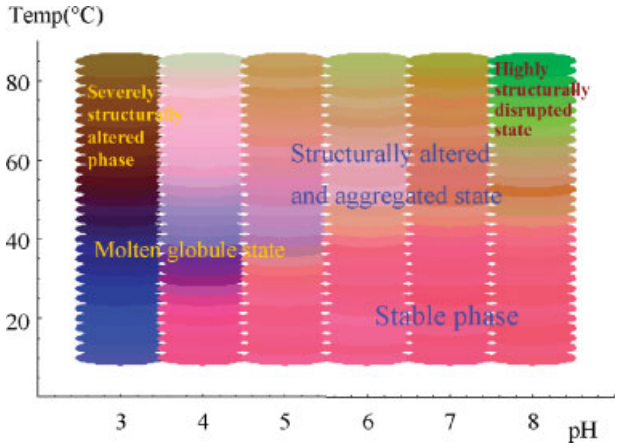

Figure 2. Phase diagram of rPA based on intrinsic, ANS dye-binding fluorescence, and CD results. Distinct phases are observed: (1) most stable phase [red-colored region in the lower right-hand corner]; (2) molten globule-like state [blue/purple area at pH 3, <45°C, pH 4, 25–40°C, and pH 5, 30–45°C]; (3) severely structurally altered phase [dark brown area at pH 3, >45°C]; (4) structurally altered and aggregated state [light purple ~ light brown region at pH 4–7, >50°C and pH 8, 50–65°C]; (5) highly structurally disrupted form [green area at pH 8, >65°C]. Blocks of continuous color represent single phases, conditions under which the raw data-derived vectors behave similarly.

temperature and pH is shown in Figure 1E. Conformational transitions appear to follow the same patterns observed in the previous data. For example, at pH 3.0, rPA displayed significant apolar character even at 10°C, signified by a high ANS fluorescence intensity. This suggests that the protein is already structurally altered, perhaps to a molten globule state. At pH 4–8, the onset of increase in fluorescence intensity generally shifted to a higher temperature as pH increased. Also noteworthy is the decrease in the amplitude of fluorescence intensity as the pH increased, suggesting less binding of ANS to rPA at increasing pH. These findings again demonstrate that the optimal pH range for rPA stability is 7–8. Moreover, the ANS fluorescence results are consistent with the presence of molten globule states at intermediate temperatures (Tab. 2).

An Empirical Phase Diagram

A phase diagram was constructed using the results of ANS fluorescence intensity, the intrinsic tryptophan fluorescence center of mass and the CD intensity. Such a color map provides information regarding the state of rPA's secondary and tertiary structures as a function of both pH and temperature. This mathematical approach provides a useful tool with which to interpret large quantities of data from different biophysical techniques for wide pH and temperature ranges. Each color represents a different physical state of the protein. Thus, a region of consistent color corresponds to an identifiable state while abrupt color differences correspond to changes in protein states (i.e., phase boundaries). The nature of each phase can be identified by simultaneously looking at the original CD and fluorescence thermal melt spectra. We emphasize the empirical nature of such diagrams (no equilibrium between states is implied) and their primarily practical utility as representations of protein behavior in solution.

In the phase diagram for rPA (Fig. 2), drastic color contrast clearly reflects changes in conformational stability over a variety of pH and temperature ranges. According to the previous discussion, the red-colored region in the lower, right-hand corner of the diagram can be identified as the phase of maximum stability (i.e., the "native" state of the protein). A second phase (blue/purple) is observed at pH 3 at temperatures below 45°C and also appears to encompass pH 4 & 5 at temperatures between 25–40°C and 30–45°C, respectively. As discussed previously, this state possesses significant molten globule character. At higher temperatures at pH 3, rPA rapidly enters another state reflected by the dark brown color. This phase represents a severely structurally altered state of the protein. In the pH range of 4–7 at high temperatures (>50°C) and pH 8 (50–65°C), the light purple to light brown zone corresponds to the structurally altered and aggregated states,

which were identified previously in the UV turbidity studies. At pH 8, yet another phase exists at >65°C, which we speculate may correspond to an even further structurally disrupted form. This phase diagram serves to identify the boundaries at which changes occur and can be used to select conditions for the development of a high-throughput stabilizer screening assay and for formulation optimization.

Screening for Stabilizers

As shown in Figure 1A, aggregation is a prominent pathway of physical degradation for rPA. Therefore, a turbidity-based high throughput screening assay was developed to examine the ability of various GRAS excipients to inhibit the aggregation of rPA. Based on the phase diagram, screening was performed at pH 5 and 37°C. These conditions were chosen based on the intrinsic marginal stability of rPA at this pH and temperature. The conditions serve well the requirements of accelerated stability testing since the protein readily aggregates at this pH and temperature. At the same time, they are sufficiently moderate to be relevant to phenomena occurring under typical pharmaceutical storage conditions. Figure 3 shows a representative plot of aggregation versus time for rPA at 37°C with and without the presence of three stabilizing excipients (malic acid, Tween-20, and sodium citrate). Several compounds exhibited a significant (>50%) ability to suppress rPA aggregation (Tab. 3). In contrast, pluronic F-68 and dextran T-40 at certain concentrations induced rPA aggregation. The disaccharide trehalose was found to be one of the most effective aggregation inhibitors. The extent of inhibition of rPA aggregation was also concentration-dependent (Fig. 4). In this case, 5% or higher concentrations of trehalose elicited ≥50% inhibition of rPA aggregation.

After certain aggregation inhibitors were identified, a number were further studied for their effects on the conformational stability of rPA using CD (Fig. 5A) and intrinsic Trp fluorescence (Fig. 5B). The data indicate that citrate, mannitol, and trehalose stabilize both the secondary and tertiary structure of rPA against thermal perturbation while Brij 35 has little effect. Trehalose produced the greatest stabilization, as demonstrated by a significant elevation in T_m of 10°C in both CD and intrinsic fluorescence studies.

Formulation of Anthrax Dry Powder Vaccine

Having identified certain conditions that lead to enhanced stability of rPA in the liquid state, we prepared and characterized dry powder formulations based on these findings. These powders have been previously shown to protect rabbits from inhalational anthrax challenge[27] (Tab. 1). The powders were produced by either FD or SFD processes. The lyophilized cakes did not display any evident collapse or obvious shrinkage. The

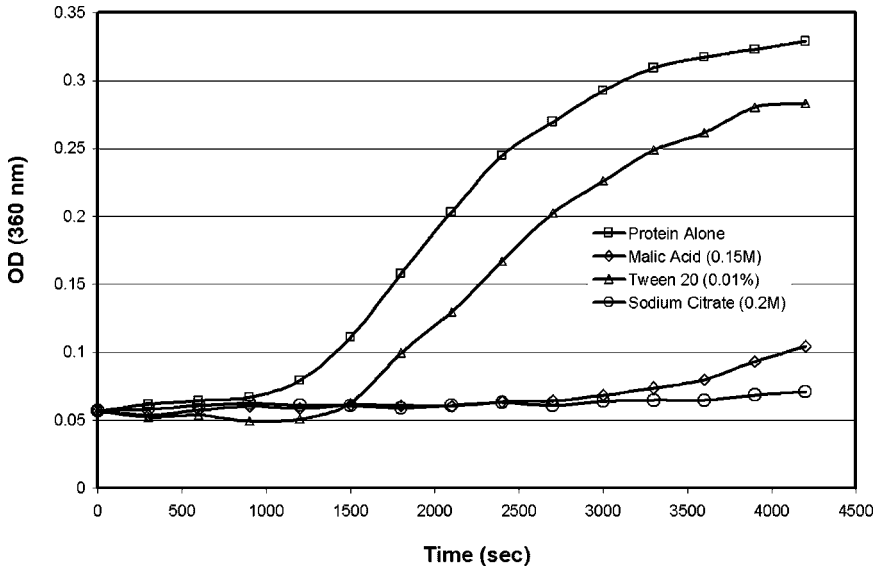

Figure 3. Aggregation of rPA in the presence and absence of excipients including 0.15 M malic acid, 0.01% Tween 20, and 0.2% sodium citrate.

Table 3. Effect of Various GRAS Excipients on rPA Aggregation

Excipient	Molar Ratio (Excipient: rPA); Molarity (Excipient) or wt. Percent (Excipient)	% Inhibition*
Brij 35	0.10%	99
Sodium citrate	0.2 M	95
Sodium citrate	0.1 M	94
Trehalose	20.00%	94
Malic acid	0.15 M	83
Trehalose	10.00%	78
Brij 35	0.05%	72
Tween 80	0.10%	46
Brij 35	0.01%	41
Tween 80	0.05%	23
Tween 20	0.05%	22
Tween 80	0.01%	17
Tween 20	0.01%	16
Tween 20	0.10%	14
Dextran T40	0.1	12
Dextran T40	2.5	1
Brij 35	0.10%	0
Dextran T40	1.0	−3
Pluronic F-68	0.10%	−12
Pluronic F-68	0.05%	−14
Pluronic F-68	0.01%	−19

*Values are ± 3%.

SFD powder consisted of highly porous particles with an uneven surface (Fig. 6) and a bulk density of approximately 0.04 g/cc. The average particle size was approximately 70 μm, a size appropriate for deposition in the nasal cavity and large enough to minimize chances of entry into the bronchioles or deep lungs. The lyophilized cake was converted into a powder by ball milling. Additionally, to study the potential utility of bioadhesion, selected formulations were prepared containing dry chitosan, which was blended with rPA/CpG/trehalose powders prior to filling into IN delivery devices for the animal testing described previously.[27]

Effect of SFD on rPA Stability

In an attempt to determine any changes in rPA integrity that might occur due to the SFD process, samples were collected at various stages, including solution preparation, spraying, instant freezing of sprayed droplets, and SFD. The dried powder was reconstituted for SDS–PAGE analysis (Fig. 7), and SEC-HPLC (Fig. 8). Under both reducing and nonreducing conditions, samples from all four stages appeared as a predominant, intense 83 kDa band identical to the fresh rPA standard. The CpG oligonucleotide did not have any noticeable effect. A variety of physical studies also found no evidence of interaction between the protein and oligonucleotide (data not shown). Two weaker bands of lower molecular weight appeared at approximately 65 kDa and 58 kDa. Comparing the intensity of the bands, these impurities represent a concentration of less than 5% of rPA monomer and exist equally in the rPA standard

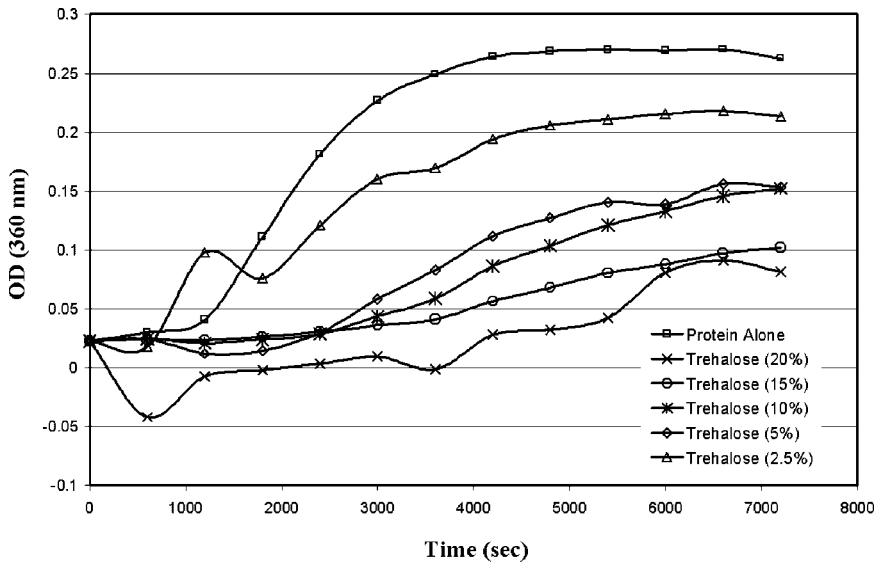

Figure 4. Protection against rPA aggregation by trehalose at six different concentrations: 0%, 2.5%, 5%, 10%, 15%, and 20%.

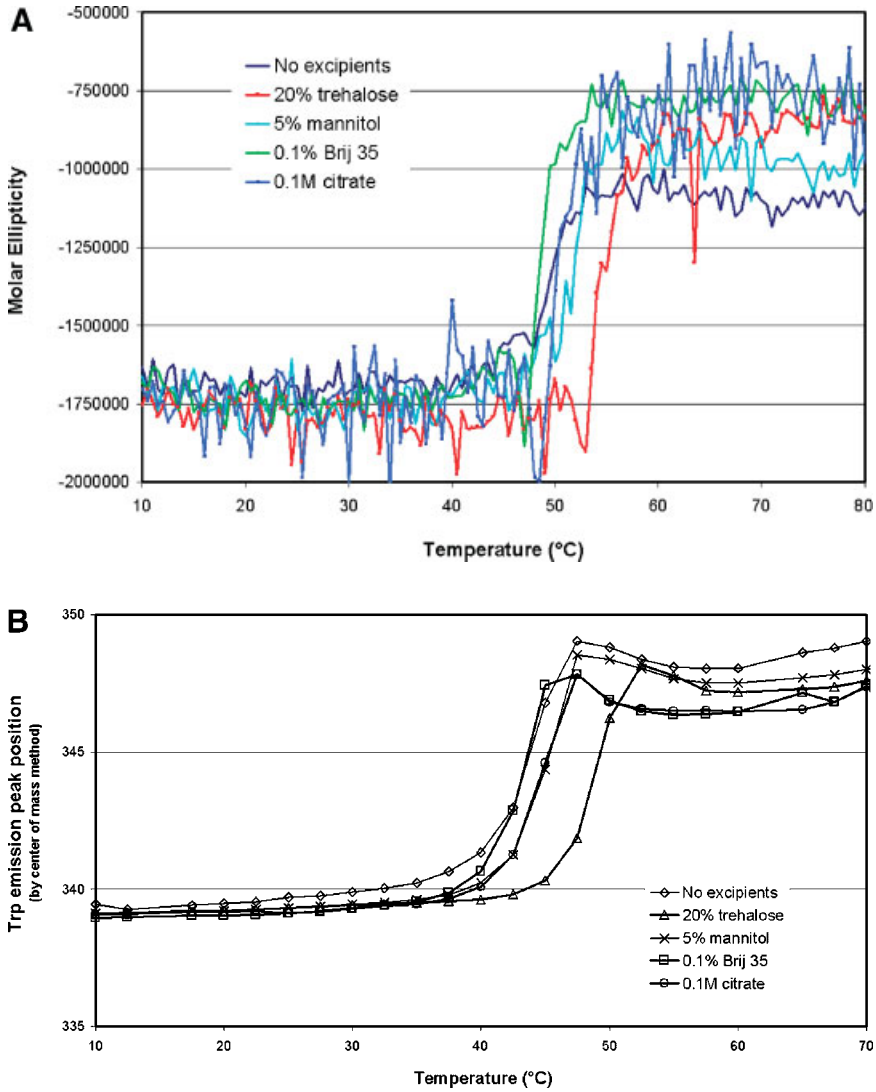

Figure 5. Increase in rPA thermal transition temperature in the presence of trehalose compared to several other excipients as determined by CD (A) and Trp fluorescence (B).

and all processed samples. No aggregation bands were observed under nonreducing conditions, suggesting that covalent disulfide linkages were not formed as a result of the large air–liquid interface present during the spaying process. Thus, this analysis suggests that the SFD process yielded native-like rPA upon reconstitution.

In SEC chromatograms (Fig. 8), rPA and CpG peaks were well resolved and accurately quantified. The SFD powder and the liquid prior to the SFD process showed comparable rPA and CpG retention times as well as similar peak areas. No additional aggregation or degradation was detected. Therefore, retention of rPA integrity was also supported by SEC-HPLC studies.

Storage Stability Studies of Anthrax Vaccine Formulations under Accelerated Conditions

Stability testing was conducted at 25 and 40°C. The higher temperature was chosen as an accelerated stability condition, to rapidly obtain data for extrapolation to longer term storage at lower temperatures. Stability at ambient conditions is highly desirable for convenience of use, potential for rapid dissemination after a bioterror attack, and to minimize costs for maintenance of a vaccine stockpile. The SFD powder anthrax vaccine consists of rPA, CpG, trehalose, and trace amounts of buffer salts. The liquid formulation was of the same composition and was tested along

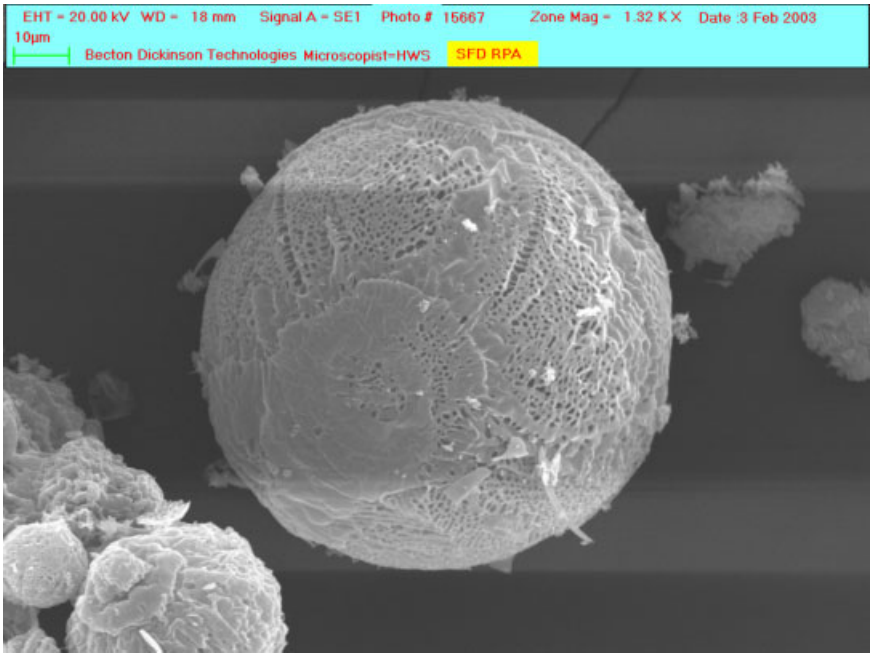

Figure 6. SEM of spray freeze dried rPA anthrax vaccine powder. [Color figure can be seen in the online version of this article, available on the website, www.interscience.wiley.com.]

with the powder for comparison and as a control. During incubation at both 25 and 40°C, powder samples maintained their physical appearance as a light powder and could be rapidly reconstituted into clear solutions at each time point.

At 25°C (Fig. 9A), the stability of the powder rPA was not adversely affected throughout the 15 days of incubation since over 90% intact monomer content was found at each time point by SEC. The molecular weight (83 kDa) of the monomer

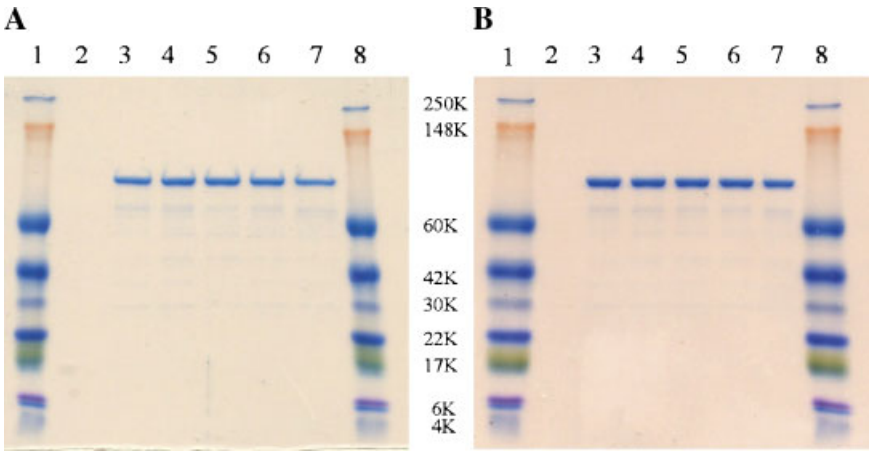

Figure 7. Retention of rPA integrity throughout the spray freeze drying process as determined by SDS–PAGE under reducing conditions (A) and nonreducing conditions (B). Lanes 1 and 8, MW marker; lane 2, CpG Std; lane 3, rPA Std; lane 4, rPA/CpG/trehalose solution; lane 5, solution sprayed from nozzle; lane 6, instant freezing of sprayed droplets in liquid nitrogen; lane 7, reconstituted spray freeze dried powder. [Color figure can be seen in the online version of this article, available on the website, www.interscience.wiley.com.]

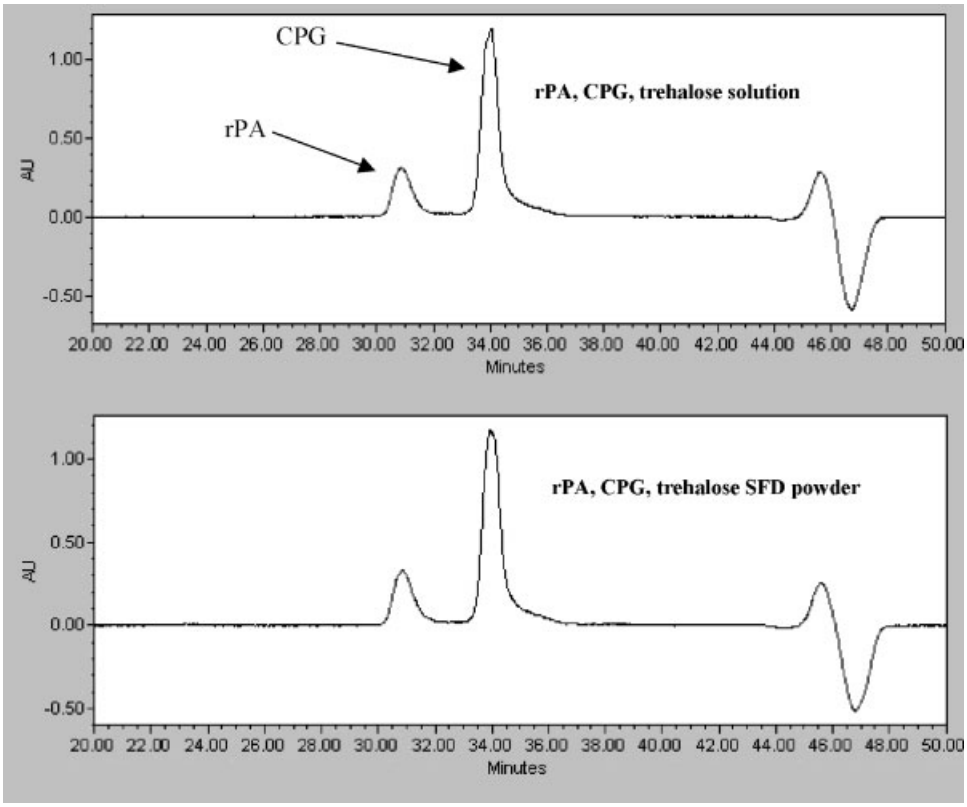

Figure 8. Retention of rPA stability after spray freeze drying as determined by SEC-HPLC.

peak was confirmed by light scattering. In contrast, the liquid formulation displayed significant degradation over the course of the study. The residual stability of the liquid at day 15 was found to be only 15% (Fig. 9A).

At 40°C (Fig. 9B), the powder retained over 90% stability during the entire time course of 29 days. The liquid formulation, however, completely lost its monomer content in 1 day. The intact rPA monomer peak was below the low level of quantification of the SEC method after only 24 h incubation and remained undetectable throughout the study. Retention of stability in the powder formulation at 40°C suggests that the powder may be successfully stored for long periods at room temperature. Removal of the need for the cold chain during storage and transportation along with the potential for self-administration using IN delivery may provide significant advantages for biodefense mass immunization.

The SEC results correlate closely with the findings of SDS–PAGE under reducing conditions. For example, on day 0, both liquid and powder formulations were identical to the fresh rPA standard (Fig. 10A). On day 1, at 40°C, the intact rPA monomer band in the liquid formulation was much lighter than the rPA standard in intensity and more prominent degradation bands appeared between 30 and 42 kDa (Fig. 10B). It should be noted that the total intensity of all bands for the solution sample was still lower than that of the standard, indicating that additional smaller fragments less than 4 kDa may have been generated. The liquid formulation continued to degrade further after day 1. On day 3, the 83 kDa rPA monomer band was completely absent and only a few bands of faded intensity at 40 kDa and lower were apparent (Fig. 10C). For the SFD powder formulation under the same conditions, the samples appear unaltered compared to the rPA standard (Fig. 10A–C). This pattern persisted through day 29. At 25°C, the degradation of rPA in the liquid formulation appeared to follow the same pattern as that at 40°C except that the deterioration process was more gradual, that is, it took longer to reach the same degree of degradation at 25°C than at 40°C. As expected, the powder at 25°C retained the same characteristics as the intact standard.

To gain a better understanding of the effect of temperature on the liquid stability of rPA and to

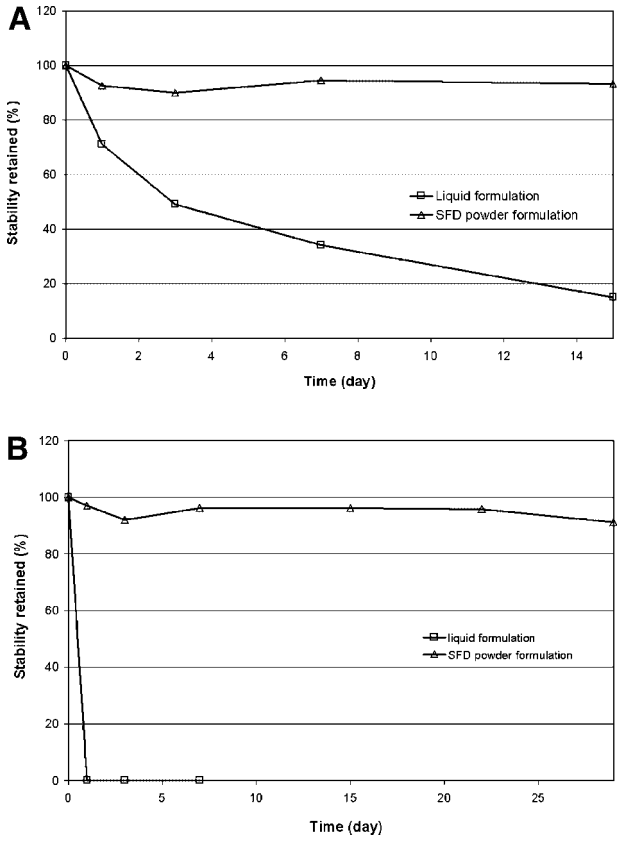

Figure 9. Storage stability of rPA liquid and spray freeze dried powder at 25°C (A) and 40°C (B) determined by SEC-HPLC.

estimate whether the liquid could be stored refrigerated instead of frozen, additional liquid stability testing was performed at 20°C and 30°C. Figure 11A shows loss of intact rPA for the liquid formulation as a function of time at four temperatures (20°C, 25°C, 30°C, and 40°C) as determined by SEC-HPLC. As predicted, the rate of deterioration increased as the temperature was elevated, and decreased with time. The stability profile was fitted using a first order model (Fig. 11B) where the log percentage of intact rPA remaining was plotted against time. This simple model fits reasonably well for the experimental data at 20°C and 25°C with an $R^2 > 0.96$. The 30°C profile had only three time points during the period of rPA degradation, which could account for the poorer fit ($R^2 = 0.82$). Based on these results, the liquid formulation should be kept frozen during long-term storage, at least under these formulation conditions.

SUMMARY AND CONCLUSIONS

We previously reported that IN anthrax vaccine powders provided complete protection of rabbits against anthrax lethal aerosol challenge. The formulation development for this vaccine powder is comprehensively described in this study. This work first investigated the physical stability of

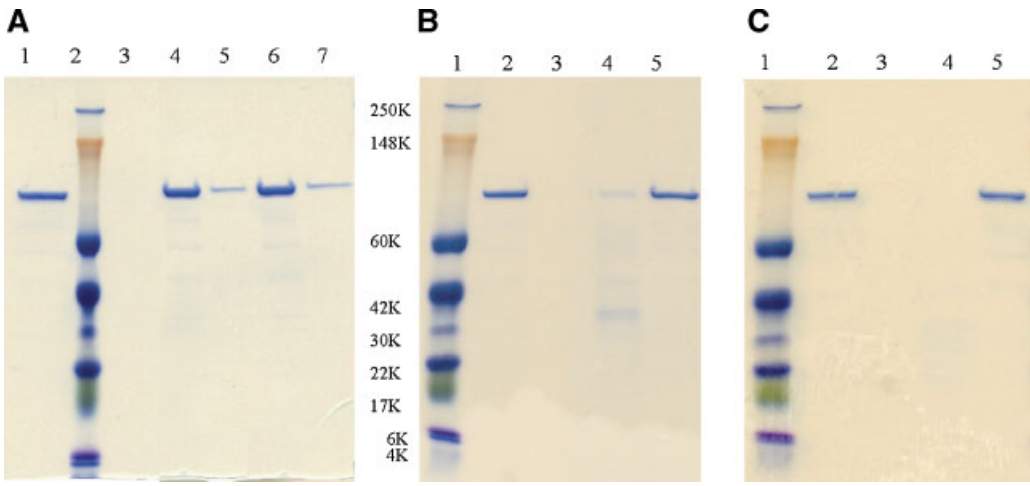

Figure 10. Degradation of the liquid formulation at 40°C determined by SDS–PAGE under reducing conditions on day 0 (A; lane 1, 2 μg rPA Std; lane 2, MW marker; lane 3, 2 μg CpG Std; lane 4 and 5, liquid formulation containing rPA 2 μg and 0.5 μg, respectively; lane 6 and 7, SFD powder formulation containing rPA 2 μg and 0.5 μg, respectively), day 1 and day 3 (B and C; lane 1, MW marker; lane 2, rPA Std 1.5 μg; lane 3, CpG Std 1.5 μg; lane 4, liquid formulation containing rPA 1.5 μg; lane 5, SFD powder formulation containing rPA 1.5 μg). [Color figure can be seen in the online version of this article, available on the website, www.interscience.wiley.com.]

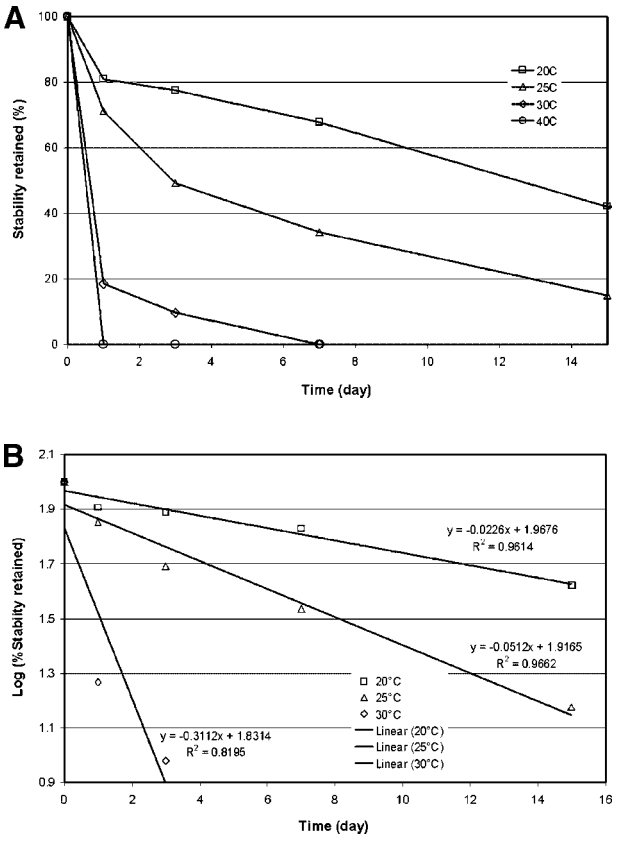

Figure 11. Degradation profiles of the liquid formulation at 20, 25, 30, and 40°C as determined by SEC-HPLC (A) and the data fit to 1st order kinetics (B).

rPA in solution as a function of pH and temperature. The stabilizing effect of GRAS excipents on rPA aggregation and loss of conformational stability was determined. Based on these findings, anthrax vaccine powders including SFD or FD dosage forms were prepared at pH 7–8 with trehalose as a stabilizer and bulking agent. The stability of rPA was retained after powder processing. The dry powder also maintained protein integrity under both ambient and accelerated aging temperatures for approximately 1 month while the liquid formulation showed rapid degradation. Such degradation appears to follow first order kinetics.

Based on these studies, stable IN powder formulations of rPA were developed as a potential alternative to heat-labile liquid formulations and conventional parenteral delivery by injection. Combination of this powder formulation with the noninvasive delivery platform described previously[27,31] could greatly improve the viability of mass immunization for this important pathogen.

ACKNOWLEDGMENTS

The authors thank Harry Sugg for performing electron microscopy on powder samples, and Pat McCutchen and Linda Tingen for administrative assistance in preparing the manuscript. Financial support was provided by funding from the U.S. Army Medical Research and Material Command, agreement number DAMD17-03-2-0037.

REFERENCES

1. Oncu S, Sakarya S. 2003. Anthrax—An overview. Med Sci Monit 9:RA276–RA283.
2. Flick-Smith HC, Eyles JE, Hebdon R, Waters EL, Beedham RJ, Stagg TJ, Miller J, Alpar HO, Baillie LWJ, Williamson ED. 2002. Mucosal or parenteral administration of microsphere-associated Bacillus anthracis protective antigen protects against anthrax infection in mice. Infect Immun 70:2022–2028.
3. Gupta P, Singh S, Tiwari A, Bhat R, Bhatnagar R. 2001. Effect of pH on stability of anthrax lethal factor: Correlation between denaturation and activity. Biochem Biophys Res Commun 284:568–573.
4. Bhatnagar R, Batra S. 2001. Anthrax toxin. Crit Rev Microbiol 27:167–200.
5. Quinn CP, Turnbull PC. 1998. Anthrax. In: Collier L, Barlow A, Sussman M, editors. Topley and Wilson's microbiology and microbial infections, 9th edition. London, UK: Arnold.
6. Tan Y, Hackett NR, Boyer JL, Crystal RG. 2003. Protective immunity evoked against anthrax lethal toxin after a single intramuscular administration of an adenovirus-based vaccine encoding humanized protective antigen. Hum Gene Ther 14:1673–1682.
7. Abrami L, Lindsay M, Parton RG, Leppla SH, van der Goot FG. 2004. Membrane insertion of anthrax protective antigen and cytoplasmic delivery of lethal factor occur at different stages of the endocytic pathway. J Cell Biol 166:645–651.
8. Arora N, Klimpel KR, Singh Y, Leppla SH. 1992. Fusions of anthrax toxin lethal factor to the ADP-ribosylation domain of Pseudomonas exotoxin A are potent cytotoxins which are translocated to the cytosol of mammalian cells. J Biol Chem 267: 15542–15548.
9. Chauhan V, Bhatnagar R. 2002. Identification of amino acid residues of anthrax protective antigen involved in binding with lethal factor. Infect Immun 70:4477–4484.
10. Pezard C, Berche P, Mock M. 1991. Contribution of individual toxin components to virulence of Bacillus anthracis. Infect Immun 59:3472–3477.

11. Hanna P. 1999. Lethal toxin actions and their consequences. J Appl Microbiol 87:285–287.
12. Leppla SH. 1982. Anthrax toxin edema factor: A bacterial adenylate cyclase that increases cyclic AMP concentrations of eukaryotic cells. Proc Natl Acad Sci USA 79:3162–3166.
13. Hoover DL, Friedlander AM, Rogers LC, Yoon IK, Warren RL, Cross AS. 1994. Anthrax edema toxin differentially regulates lipopolysaccharide-induced monocyte production of tumor necrosis factor alpha and interleukin-6 by increasing intracellular cyclic AMP. Infect Immun 62:4432–4439.
14. Collier RJ, Young JA. 2003. Anthrax toxin. Annu Rev Cell Dev Biol 19:45–70.
15. Mogridge J, Cunningham K, Collier RJ. 2002. Stoichiometry of anthrax toxin complexes. Biochemistry 41:1079–1082.
16. Prokupek K, Dvorak R, Polacek R. 1981. Immunogenic effect of anthrax protective antigen. Vet Med (Praha) 26:279–290.
17. Ivins BE, Fellows PF, Nelson GO. 1994. Efficacy of a standard human anthrax vaccine against Bacillus anthracis spore challenge in guinea-pigs. Vaccine 12:872–874.
18. Jendrek S, Little SF, Hem S, Mitra G, Giardina S. 2003. Evaluation of the compatibility of a second generation recombinant anthrax vaccine with aluminum-containing adjuvants. Vaccine 21: 3011–3018.
19. Baillie L, Hebdon R, Flick-Smith H, Williamson D. 2003. Characterisation of the immune response to the UK human anthrax vaccine. FEMS Immunol Med Microbiol 36:83–86.
20. Reuveny S, White MD, Adar YY, Kafri Y, Altboum Z, Gozes Y, Kobiler D, Shafferman A, Velan B. 2001. Search for correlates of protective immunity conferred by anthrax vaccine. Infect Immun 69: 2888–2893.
21. Ivins BE, Welkos SL. 1986. Cloning and expression of the Bacillus anthracis protective antigen gene in Bacillus subtilis. Infect Immun 54:537–542.
22. Singh Y, Ivins BE, Leppla SH. 1998. Study of immunization against anthrax with the purified recombinant protective antigen of Bacillus anthracis. Infect Immun 66:3447–3448.
23. Clinicaltrials.gov website www.clinicaltrials.gov/ct/show/NCT00057525. ed.
24. Tebbey PW, Scheuer CA, Peek JA, Zhu D, LaPierre NA, Green BA, Phillips ED, Ibraghimov AR, Eldridge JH, Hancock GE. 2000. Effective mucosal immunization against respiratory syncytial virus using purified F protein and a genetically detoxified cholera holotoxin, CT-E29H. Vaccine 18:2723–2734.
25. Papp Z, Babiuk LA, Baca-Estrada ME. 1999. Antigen-specific cytokine and antibody isotype profiles induced by mucosal and systemic immunization with recombinant adenoviruses. Viral Immunol 12:107–116.
26. Isaka M, Yasuda Y, Taniguchi T, Kozuka S, Matano K, Maeyama J, Morokuma K, Ohkuma K, Goto N, Tochikubo K. 2003. Mucosal and systemic antibody responses against an acellular pertussis vaccine in mice after intranasal co-administration with recombinant cholera toxin B subunit as an adjuvant. Vaccine 21:1165–1173.
27. Mikszta JA, Sullivan VJ, Dean C, Waterston AM, Alarcon JB, Dekker JP, Brittingham JM, Huang J, Hwang CR, Ferriter M, Jiang G, Mar K, Saikh KU, Stiles BJ, Roy CJ, Ulrich RG, Harvey NG. 2005. Protective immunization against inhalational anthrax: A comparison of minimally-invasive delivery platforms. J Infect Dis 191:278–288.
28. Kueltzo LA, Ersoy B, Ralston JP, Middaugh CR. 2003. Derivative absorbance spectroscopy and protein phase diagrams as tools for comprehensive protein characterization: A bGCSF case study. J Pharm Sci 92:1805–1820.
29. Klinman DM. 2003. CpG DNA as a vaccine adjuvant. Expert Review of Vaccines 2:305–315.
30. Kueltzo LA, Middaugh CR. 2003. Structural characterization of bovine granulocyte colony stimulating factor: Effect of temperature and pH. J Pharm Sci 92:1793–1804.
31. Huang J, Garmise RJ, Crowder TM, Mar KM, Hwang CR, Hickey AJ, Mikszta JM. 2004. SVJ 2004. A novel dry powder influenza vaccine and intranasal delivery technology: Induction of systemic and mucosal immune responses in rats. Vaccine 23:794–801.
32. Radha C, Salotra P, Bhat R, Bhatnagar R. 1996. Thermostabilization of protective antigen—The binding component of anthrax lethal toxin. J Biotechnol 50:235–242.
33. Buchner J, Renner M, Lilie H, Hinz HJ, Jaenicke R, Kiefhabel T, Rudolph R. 1991. Alternatively folded states of an immunoglobulin. Biochemistry 30: 6922–6929.
34. Mayo KH, Barker S, Kuranda MJ, Hunt AJ, Myers JA, Maione TE. 1992. Molten globule monomer to condensed dimer: Role of disulfide bonds in platelet factor-4 folding and subunit association. Biochemistry 31:12255–12265.
35. Tanksale A, Ghatge M, Deshpande V. 2002. Alpha-crystallin binds to the aggregation-prone molten-globule state of alkaline protease: Implications for preventing irreversible thermal denaturation. Protein Sci 11:1720–1728.
36. Karlsson M, Martensson LG, Olofsson P, Carlsson U. 2004. Circumnavigating misfolding traps in the energy landscape through protein engineering: Suppression of molten globule and aggregation in carbonic anhydrase. Biochemistry 43:6803–6807.
37. Asghari SM, Khajeh K, Ranjbar B, Sajedi RH, Naderi-Manesh H. 2004. Comparative studies on

trifluoroethanol (TFE) state of a thermophilic alpha-amylase and its mesophilic counterpart: Limited proteolysis, conformational analysis, aggregation and reactivation of the enzymes. Int J Biol Macromol 34:173–179.
38. Mazon H, Marcillat O, Forest E, Smith DL, Vial C. 2004. Conformational dynamics of the GdmHCl-induced molten globule state of creatine kinase monitored by hydrogen exchange and mass spectrometry. Biochemistry 43:5045–5054.
39. Almstedt K, Lundqvist M, Carlsson J, Karlsson M, Persson B, Jonsson BH, Carlsson U, Hammarstrom P. 2004. Unfolding a folding disease: Folding, misfolding and aggregation of the marble brain syndrome-associated mutant H107Y of human carbonic anhydrase II. J Mol Biol 342:619–633.